MilliMobile: An Autonomous Battery-free Wireless Microrobot

Kyle Johnson[1†], Zachary Englhardt[1†], Vicente Arroyos[1†]
Dennis Yin[2], Shwetak Patel[1,2], Vikram Iyer[1]
[1] Paul G. Allen School of Computer Science & Engineering, University of Washington
[2] Department of Electrical and Computer Engineering, University of Washington
[†] Co-primary Student Authors

ABSTRACT

We present MilliMobile: a first of its kind battery-free autonomous robot capable of operating on harvested solar and RF power. We challenge the conventional assumption that motion and actuation are beyond the capabilities of battery-free devices and demonstrate completely untethered autonomous operation in realistic indoor and outdoor lighting as well as RF power delivery scenarios. We show first that through miniaturizing a robot to gram scale, we can significantly reduce the energy required to move it. Second, we develop methods to produce intermittent motion by discharging a small capacitor (47-150 µF) to move a motor in discrete steps, enabling motion from as little as 50 µW of power or less. We further develop software defined techniques for maximizing power harvesting. MilliMobile operates in the optimal part of the charging curve by varying the charging time to achieve maximum speeds of up to 5.5 mm/s.

The MilliMobile prototype has a 10x10 mm chassis and weighs less than 1.1 g. Our robot can carry payloads 3 times its own weight, and only experiences a 25% reduction in speed when carrying a 1 g payload. We demonstrate operation on 10 different surfaces ranging from wood and concrete to compact soil. We further show the ability to cold-start and move in light conditions as low as 20 W/m^2 and -10 dBm of RF power. In addition to operating on harvested power, our robot demonstrates sensor and control autonomy by seeking light using onboard photodiodes, and can transmit sensor data wirelessly to a base station over 200 m away.

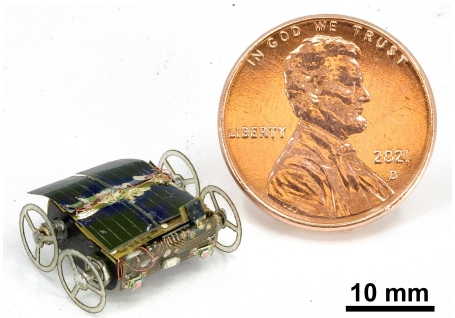

Figure 1: MilliMobile- an autonomous battery-free, wireless robot shown next to a US penny for scale. Video: https://homes.cs.washington.edu/~vsiyer/millimobile.html

CCS CONCEPTS

• **Computer systems organization** → **Embedded hardware**; **Robotic autonomy**; • **Hardware** → *Sensor devices and platforms*; *Wireless devices.*

KEYWORDS

battery-free robots, power harvesting, autonomous sensing

ACM Reference Format:
Kyle Johnson[1†], Zachary Englhardt[1†], Vicente Arroyos[1†], Dennis Yin[2], Shwetak Patel[1,2], Vikram Iyer[1]. 2023. MilliMobile: An Autonomous Battery-free Wireless Microrobot. In *The 29th Annual International Conference on Mobile Computing and Networking (ACM MobiCom '23), October 2–6, 2023, Madrid, Spain.* ACM, Madrid, MD, Spain, 16 pages. https://doi.org/10.1145/3570361.3613304

1 INTRODUCTION

Robotic sensor networks have transformative potential for numerous applications. Unlike fixed IoT nodes, the ability for a sensor to move enables a single robot to sample larger areas and dynamic spatial reconfiguration of networks. Such robots could perform infrastructure inspection on roadways, bridges, and railroads, track inventory on warehouse shelves, measure environmental conditions for indoor farms, or take measurements in industrial scenarios with toxic chemicals or strong electromagnetic fields. Mobility also enables seeking out signal sources such as fires or gas leaks [15, 17, 61]. Autonomous robotic sensor nodes could even automatically

ACM MobiCom '23, October 2–6, 2023, Madrid, Spain

ACM ISBN 978-1-4503-9990-6/23/10.
https://doi.org/10.1145/3570361.3613304

Millimeter-scale Robots	Battery Free Mobility	Power Autonomy (untethered)	Control Autonomy & Sensing	Communication Link, Range	Mass (g)	Characteristic Length (mm)	Min. Power While Moving (µW)
Kilobot	-	✓	✓	Infrared LED & Photodiode, (0.1 m)	36	33	12,000
HAMR-F	-	✓	✓	802.15.4, (5 m)	2.79	45	423,000
RoACH	-	✓	-	IRDA Infrared, (1 m)	2.4	30	440,000
Soft Millirobot Carried-on	✓	- *	-	NFC (0.09 m)	>0.05*	30	203*
Alice	-	✓	-	RF 433 MHz, (10 m)	5	21	4,000
Bipedal eBiobot	✓	- *	-	NFC (0.09 m)	>5*	35	-
Laser-powered Microrobot	✓	✓	-	-	0.1	18	2,500
MilliMobile	✓	✓	✓	BLE (200 m)	1.09	11	50

Figure 2: Comparison of millimeter-scale robots Kilobot [59], HAMR-F [21], RoACH [24], Soft Millirobot Carried-on [45], Alice [8], Bipedal eBiobot [41], Laser-powered Microrobot [6], and MilliMobile (this work). *Untethered power autonomy denotes onboard power harvesting operational at >1 m, excluding magnetic and near field designs [41, 45]. These designs do not specify power and mass, estimates were extrapolated based on available data and related works.

disperse themselves to avoid manual deployment, a major barrier in domains such as precision agriculture.

Robots however require significantly more energy for their mechanical propulsion than a fixed IoT node [19]. Combined with the energy density of current batteries [64], this results in lifetimes of minutes to hours compared to years for fixed sensors. Further, this restricts the area a robot can traverse and imposes significant maintenance costs to change or recharge batteries. Batteries also have significant environmental costs. Lithium batteries, which are ubiquitous in mobile devices pose significant ecotoxicity and human health concerns at end of life disposal due to high levels of lead, cobalt, chromium, and thallium [37]. Additionally, battery manufacturing also has significant environmental impacts and requires for critical minerals [3, 65].

In this work we ask a seemingly radical question, is it possible to design an *autonomous, battery-free robot*? We challenge the conventional assumption that motion is inherently energy-expensive, and explore co-optimizing size, weight and power to create MilliMobile: a first of its kind battery-free autonomous robot that can operate on harvested solar and RF power (see Fig 1). Our programmable, gram scale, wheeled robot measures ~1 cm^2 and can cold-start and move with 50 µW of power or less (see Fig 2). This enables many practical power harvesting scenarios with both indoor and outdoor lighting as low as 20 W/m^2, and RF power as low as -10 dBm to operate within safety limits. MilliMobile supports a variety of sensor payloads up to three times its own weight, and demonstrates autonomous operation by seeking out light sources. We compare the MilliMobile to other millimeter-scale robots in Fig 2, highlighting the novelty of battery-free power and control autonomy at the ~1 cm^2 size.

Achieving this goal requires addressing a number of challenges. First and foremost, power harvesting sources produce tens of microwatts to a maximum of a few milliwatts of power in realistic scenarios. High efficiency solar cells produce a maximum of 6 mW/cm^2 in bright outdoor light and RF transmit powers are limited to 1 mW/cm^2 for safety. Moreover, a truly autonomous robot must be able to carry its harvester onboard (untethered power autonomy) and move independently in a variety of situations (sensing and control autonomy) [62]. This eliminates kinetic and thermal energy harvesting used in wearables [12], and prevents the use of power expensive actuators used in prior robots [32, 41, 49, 54].

Energy and Scaling analysis. To understand how these challenges relate to the energy required to move a robot of mass m to a target velocity v we analyze its kinetic energy $KE = \frac{1}{2}mv^2$. The linear scaling of energy with mass suggests a ~1 g, robot should require <1 mJ. This demonstrates the potential for using miniaturization to develop a robotic system compatible with the microwatts to milliwatts available in practical power harvesting scenarios. We therefore target a robot design weighing ~1 g.

Further, we observe that energy harvesting for robots fundamentally favors small scale. A cubic robot with characteristic length ℓ has surface area $SA = 6\ell^2$, volume $V = \ell^3$, and mass $m = \rho V$ where ρ is density. We observe that $SA \propto \ell^2$, $V \propto \ell^3$, and $m \propto \ell^3$. Battery-free designs favor high SA-to-V ratios that maximize their harvester area which scales with ℓ^2, versus the power required to move their mass which scales with ℓ^3 [18]. This analysis supports miniaturization for developing battery-free robots and we therefore explore the design space of small robots with ℓ of ~1 cm.

Intermittent motion. Reducing the robot's mass lowers the energy required to move, however we also need a mechanism to produce motion in a small form factor. This raises a second challenge as even small, sub-gram motors require tens to hundreds of milliwatts to spin continuously [1]. While continuous motion is common in wheeled robots and drones, this is not the case in most natural systems. Legged locomotion in animals for example occurs in discrete steps. Inspired by this, we explore a new paradigm of *intermittent motion* for moving battery free robots.

Developing this physical analog of intermittent computing requires producing discrete "atomic" motions. This necessitates buffering energy in our small form factor from variable power sources, and a transducer to convert that energy into mechanical motion. The energy stored in a capacitor is given by $\frac{1}{2}CV^2$. Charging a ~100 μF capacitor to 5 V is therefore sufficient to store over 1 mJ of energy.

Based on this intuition, we perform a simple experiment and observe a surprising result: discharging a 100 μF capacitor directly into a small eccentric rotating mass (ERM) vibration motor is sufficient to overcome inertia and resistive losses and produce discrete revolutions of a 450 mg mass.

Contributions. Building on this primitive, we design a fully functional gram-scale battery-free wireless robot measuring ~1 cm^2. Unlike prior robots that use magnetic fields limited to centimeter ranges [50, 55, 66], or high powered lasers [2, 33] and RF transmitters [54], we demonstrate the first autonomous, completely untethered robot that requires orders of magnitude less harvested power. Using <100 μW of harvested ambient power MilliMobile can traverse distances of 10.8 meters within 60 minutes. We summarize the key contributions of our work below.

- **MilliMobile platform.** We develop a first of its kind gram scale, autonomous, programmable robotic sensing platform that can move with <100 μW of harvested power. Our robot is complete with power harvesting, wireless connectivity, and sensors for light, temperature and humidity.
- **Battery-free motion.** We demonstrate robust battery-free operation of our robot using solar power in both outdoor and indoor lighting as well as with RF power. Our robot can move at a maximum speed of 5 mm/s, carry payloads up to 3 times its weight, and move on a variety of surfaces ranging from concrete to carpet.
- **Optimizing intermittent motion.** We introduce the concept of intermittent motion develop optimized sub-gram power harvesting and actuation hardware. Additionally, we develop a software defined maximum power point tracking strategy using variable length capacitor charge times to co-optimize power harvesting with robot speed.
- **Autonomous operation.** In addition to power autonomy, our robot is the first at this scale to demonstrate sensing and control autonomy as well. We show one demonstration of this by using the onboard microcontroller to sample a series of photodiodes and an onboard control algorithm allowing the robot to steer itself toward light sources.
- **Wireless connectivity.** We develop solutions for wireless connectivity between robots and to remote base station at distances over 200 m. We develop a novel battery-free synchronization strategy that leverages the robot's ability to move as a foundation for wireless robotic networking.

Link to the MilliMobile webpage and video:
https://homes.cs.washington.edu/~vsiyer/millimobile.html

2 RELATED WORK

Power harvesting robots. Achieving power autonomy for small robots has been a longstanding challenge for two decades [62]. Among the first works in this space were MEMS based structures that could be activated by light or solar power [23], however these robots were not programmable, had no sensors, no communication, highly limited payload capacity, and were not controllable. More recent chip scale robots have demonstrated potential for programmability [58] but lack radio communication and sensing. Moreover, these microscopic robots are on a dramatically different scale more than an order of magnitude smaller than our design. This makes it difficult for such robots to interact with the world, carry sensing payloads, or traverse longer distances. Attempts to create larger solar powered robots such as drones demonstrate duty cycled recharging, but cannot operate battery free [18]. These designs require hours to recharge a large battery whereas by significantly reducing the energy required for motion, our robot can repeatedly move using harvested energy in discrete steps.

Multiple works have also explored magnetic actuation for robots. These works manipulate large external magnets to directly move parts of a robot including walking robots walking robots [55, 66] driven by rotating magnetic fields and ingestible origami robots that use magnetic fields to actuate folding [46, 50, 51, 68]. These designs are fundamentally limited by distance over which magnetic fields can propagate and cannot operate at distances greater than a few centimeters. This similarly limits the feasibility of near field power harvesting [38]. Additionally many of these designs lack onboard control for truly autonomous operation.

Researchers have also explored solutions for far field wireless power with fixed high power transmitters. Optical power delivery using lasers has been explored for powering robots both large drones and insect-scale robots [2, 6, 33, 53]. While lasers can direct high power density to a small area, they are point to point links and cannot scale. Laser power delivery also requires precise positioning to deliver maximum power [26] and poses significant safety concerns of using

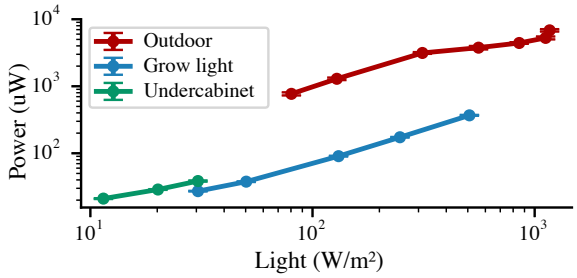

Figure 3: Solar power harvesting in various light conditions. Measurements reflect power harvested by the full robot circuit described in §3 with successful cold-start and operation.

lasers of 10s [33] to 100s of watts. High power RF power has been demonstrated for a robot [54], however this required a 30 W transmitter at 5 GHz which exceeds both the maximum power level allowable for transmission in the band as well as safety regulations. Recent works on solar power have also required unrealistically high light levels of 3 suns [31].

Insect-borne sensors. Leveraging living organisms to enable locotmotion for sensor systems is another means to overcome the challenges of mm-scale energy storage and actuation [30]. Researchers have attached sensors and tracking devices to a variety of small animals such as butterflies [42], moths [27], hornets [39, 44], and snails [7] to enable dispersal and data collection over kilometer distances. To enhance the control autonomy of these systems, insect-scale sensors have been coupled with actuators to enable steerable beetle-mounted camera modules [29]. Attempts at more precise control of insect locomotion through neural stimulation have shown some success [35] however these approaches are plagued by issues such as the eventual habituation of insect subjects to repeated stimulation. These approaches are also difficult to scale due to the limitation of raising live animals, attaching sensors manually, and reliably and consistently replicating insect behavior between tests.

In contrast to this prior work we seek to develop robots that are battery-free and can operate completely untethered and with onboard autonomous control in settings with *practical power harvesting conditions* (sunlight, indoor lighting, RF power within legal limits).

Automated sensor deployment. Recent works have begun exploring technologies for automated deployment of sensor networks and IoT devices. These include sensors that can be dropped from small drones and insects [28, 56, 57] and devices that can disperse in the wind [11, 40]. While some of these systems can operate battery free, this complementary research direction is focused on one time deployment and none of these systems are designed to move from their deployment locations. In contrast, we seek to develop truly robotic nodes that can actively move to different locations.

Millimeter scale robots. A recent review of gram-scale robots notes that despite significant work in this area there

Capacitor (part number)	Mass (mg)	Capacitance (uF)	Max Voltage (V)	ESR (ohms)	Leakage (uA)	Max Travel Distance (mm)
F980J476MSAAH1	13.3	47	6.3	1.0	3.0	2.0
F980G107MSA	13.7	100	6.3	4.0	4.0	6.0
F950J157#BAAQ2	18.0	150	6.3	0.4	9.5	15.0

Figure 4: Capacitor comparison. Travel distance measured using a 1.2 g MilliMobile and $1\ \tau$ charge time.

are no systems that demonstrate power autonomy (ability to carry a power source) as well as sensor and control autonomy (ability to carry sensors and process their data for robot control onboard) [62]. Many works in this space have focused on building robots that operate with wire tethers to demonstrate new actuators and mechanisms [5, 9, 25, 69, 70]. A small number of works have integrated onboard batteries, but they often lack control autonomy, sensing, and wireless connectivity as well [8, 24, 34, 43]. While the HAMR-F and Kilobot do incorporate these more advanced capabilities, their onboard battery capacity limits them to at best a few hours of continuous operation. [21, 60]. We are not aware of any battery-free robots to date that achieve MilliMobile's unique combination of power and control autonomy, sensing, and wireless connectivity.

Battery-free wireless sensors Battery-free devices have been explored extensively in the mobile systems community, however these works often focus on fixed sensor nodes [13, 14, 20]. We focus on robots, which introduce challenges of mechanical motion and control, as well as greater power harvesting variability as they move. For example, Capybara [10] develops software frameworks for managing tasks on battery-free systems with heterogeneous capacity and temporal constraints enabling allocation of energy bursts for radio transmissions. In this work we take these concepts a step further by developing hardware to create actuated sensing systems enabling higher energy pulses for battery-free mechanical motion, alongside algorithms that use onboard sensors to enable fully autonomous robot control operations such as source seeking.

3 SYSTEM DESIGN

3.1 Real-world power availability

We seek to design a small, battery-free robot that can operate in practical power harvesting scenarios without the dedicated high power transmitters used in prior works [2, 31, 33, 54]. Below we evaluate the power available from small, lightweight harvester prototypes in real world scenarios such as indoor and outdoor light or ceiling mounted RF transmitters as well as the voltage and current constraints of our physical robot design.

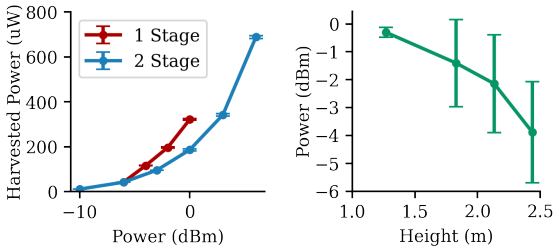

Figure 5: Left, power from 1-stage and 2-stage RF harvesting circuit. Right, receiver power versus distance from RF output.

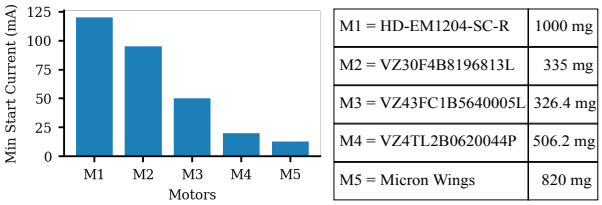

Figure 6: Starting current for various motors, including the MilliMobile's M4 motor. Motor mass values are unmodified.

Light-weight solar harvesting. To determine the amount of solar power available for intermittent motion, we design a testing setup with an array of four thin film solar cells (Microlink Devices) weighing 6 mg each. To replicate on-robot harvesting scenarios, we connect the solar cell array to two parallel 47 µF capacitors (AVX F980J476MSA) which we observe can provide enough energy to rotate a small motor. Performing this test with a real capacitor is important as the amount of power the solar cell outputs is dependent on the impedance of the load connected to it.

To measure the power we place the solar cells next to a solar power meter (TES 132) and measure the charging curve of the capacitor using a digital oscilloscope (Tektronix MDO4034) in a variety of light conditions. Specifically, we perform measurements in three scenarios to model practical power harvesting data. We perform the first test in outdoor sunlight for use in outdoor environments. Next, we perform measurements under a variable intensity grow light (Barrina BU 2000) designed for indoor farming where our robot could be used to sense microclimates around plants. Third, we measure the power available from an undercabinet light (Good Earth Lighting UC1272-WHG-24LF0) that would enable our robot to operate continuously on a desk or table.

Fig 3 shows the resulting light levels versus power available (N=3 measurements $\pm\sigma$). The data demonstrates that even in the lowest light conditions from the undercabinet light, we are able to harvest sufficient energy to overcome the capacitor's leakage current and charge (see in Fig 4). These results show the potential for our robot to operate using intermittent motion in indoor light conditions by extending the capacitor's charging time, trading-of speed for robustness.

RF power harvesting. The ability to charge capacitors at 10s of microwatts of power above opens up the possibility for RF power as well. We explore practical RF power for robots within FCC limits below including specific voltage and current constraints. We transmit a single tone at 908 MHz at 36 dBm EIRP using a USRP E310 and variable attenuator (JFW 50BR-017) connected to a power amplifier (RFMD 5110G) and an 8.2 dBi 900 MHz patch antenna (Cushcraft). We verify the output on a spectrum analyzer (MDO4034).

We design a miniaturized, modified Dickinson charge pump using SMS7630 diodes based on [63] and [30]. We first test a two stage rectifier and observe outputs of 15 V at high power which exceeds the maximum our storage capacitor can tolerate. We add an 8 V Zener diode for protection up to an RF power of 6 dBm. The results are similar to indoor lighting. Next we perform the same experiment with a single stage rectifier which does not require a Zener diode. This circuit has higher efficiency but a more limited range. Fig 5 shows the results for a one and two stage rectifier over a range of power levels.

Next we investigate power availability in realistic settings such as ceiling mounted transmitters similar to commercial RFID systems. A transmitter mounted above or around a desk could power robots across the work surface. To evaluate this, we mount the antenna described above on a variable height tripod and raise it to different heights above a wood platform. We create a millimeter scale 900 MHz wire antenna based on designs from [11, 30] and connect it to a spectrum analyzer to perform precise power measurements. To account for multipath we perform measurements at 3 locations across our ~1 m square surface. The right hand plot in Fig 5 shows these results. These results show that, even when the transmitting antenna is placed at a ceiling height of 2.4 m, the MilliMobile can harvest tens of microwatts of power, sufficient for charging the onboard capacitors while staying within RF power safety limits.

3.2 Actuating a battery free robot

The data above demonstrates the ability to harvest 10s of microwatts of power and successfully charge a capacitor but also highlight the need to minimize our system's total mass. To create a functional robot, we need to go beyond just power harvesting and couple this energy to an actuator that can produce mechanical motion. We analyze different actuator technologies to determine the optimal choice for our intermittent motion system. Many microrobot systems have used piezo actuators due to their light weight (10s of milligrams) and high efficiency [22, 48, 69]. While piezos are an attractive solution, they also require high voltages of over 200 V to operate [69]. Because the maximum voltage available from our

Component	Mass (mg)	Size: L, W, H (mm)
Chassis (folded)	29.5	10, 10, 0.35
PCB (folded)	141.5	12, 10, 6
Power Harvesting (solar cells, RF circuit)	20, 10	11, 10, 0.4 3, 3, 1
Wheels (x4)	14.0	6, 6, 0.15
Drive Motors (x2)	791.5	12, 4.7, 4.7
Bearing + Other Parts	95.5	–
Total (solar cells):	1092.0	12, 12, 6

Figure 7: Minimized mass and volume of MilliMobile components after off-the-shelf modifications.

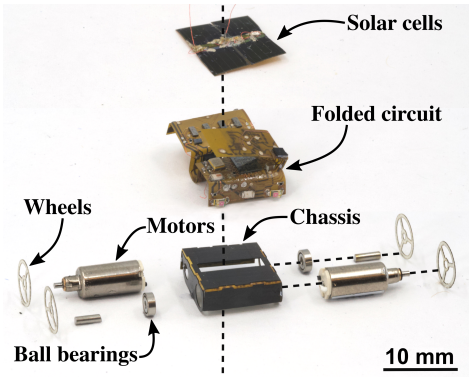

Figure 8: Exploded view of the MilliMobile robot showing the major components in relation to one another.

harvesters and capacitor is 6.3 V, these actuators would require a boost converter to increase their voltage which adds significant weight and efficiency losses [33]. Additionally, piezos operate most efficiently when driven at their resonant frequency to produce repeated motion such as wing flapping; in contrast we seek to move in discrete steps. Similarly we eliminate dielectric elastomer and other electrostatic actuators that require even higher voltages [34].

We therefore focus on low voltage (<10V) solutions such as electromagnetic or heat based actuators. Heat based actuators such as SMAs are slow and inefficient, we therfore focus on electromagnetic actuators such as motors. Small ERM vibration motors produce vibrations by rotating an off-center mass at a high rotational velocity. We note that these masses are often 0.5 to 1 g depending on the motor size and application. This shows that the motors have the ability to move 1 g and we set this as our target robot mass. Next we analyze the power requirements of these motors in Fig 6. The data shows two surprising results: first, there is high variance of over 10x between these motors. This is likely due to the application they are optimized for (higher torque vs speed) as well manufacturing tolerances such as air gaps between the magnet and motor coils. Second, at the low end there are motors that can run at 4 mA, which is even lower than the current required by many common microcontrollers and Bluetooth chips while transmitting [29].

These power requirements are similar to those of chips used in prior battery-free systems and demonstrate the feasibility of designing a battery free robot within these constraints. We choose motor M4 for our design due to its optimal power to weight ratio. This small commercially available vibration motor is designed to rotate a mass of 450 mg and the motor itself weighs 506 mg. We combine two motors and target an approximately 1 g total mass for our robot.

3.3 Intermittent motion.

The currents required by these lightweight motors are still below what is available from all but the brightest outdoor solar harvesting scenarios shown in Fig 3. Enabling battery free operation therefore requires a strategy for bridging this gap. We take inspiration from legged locomotion in natural systems and intermittent computing and propose closing this gap by moving our robot in discrete steps. Doing so however requires a component capable of storing sufficient energy to rotate a motor while supporting the robot's weight.

We evaluate a variety of capacitors as potential storage elements for intermittent motion shown in Fig 4. The key requirements for a capacitor are the ability to store sufficient energy to produce discrete motions, but also to be able to discharge this energy into a motor effectively. The force produced by a motor is proportional to its current. An important parameter for our capacitor is the equivalent series resistance (ESR) which determines the maximum current the capacitor can discharge. This parameter depends on the properties of the dielectric material used; however we note that many capacitors optimized for the lowest ESR also suffer from higher leakage currents which limits power harvesting efficiency. Similarly, optimizing for higher maximum voltage and capacitance while maintaining low ESR can also increase size. To minimize weight we select and test three capacitors with promising characteristics.

To evaluate whether these capacitors can actually move a robot we create a simple wired prototype of the chassis and motor components weighing ~1.1 g, as shown in Fig 7 and Fig 8. We place our solar cell array under the grow light setup described above and use it to charge two of each capacitor under test in parallel. We wire the motors to small, 1 mg NMOS transistors connected to ground and use this to trigger a release of current through the motors after charging the capacitors for one time constant τ (see 3.5). We use thin 43 AWG wires to connect to the robot to minimize external forces. We measure the distance traveled by the robot chassis using a ruler. Fig 4 shows that all of the capacitors are able to move the robot, including one up to 1.5x the chassis length demonstrating the feasibility of intermittent battery-free motion.

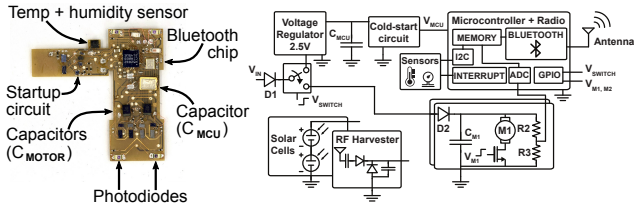

Figure 9: Left, labeled top view of foldable PCB. Right, circuit diagram showing major component blocks.

3.4 Robot mechanical design

Based on the feasibility experiments above we design a cm-scale 4-wheeled robot with a target mass of ~1 g. A breakdown of component weights are shown in Fig 7. We note that because the motors weigh approximately 500 mg each, we seek to minimize any additional weight for the rest of the system through careful selection of materials and component placement.

We designed the chassis to measure 1 cm^2 when folded up as shown in Fig 8. To minimize weight we manufacture the chassis from a single flat folded laminate consisting of carbon fiber (Toray M46J) and polyimide (Dupont Kapton). To fabricate the robot we use using laser micromachining (LPKF U4) to cut the outline and pattern the carbon fiber layers. Next we align the layers with a sheet adhesive (Pyralux FR1500) in a heat press to laminate them together and cut out the final shape (see [9] for details). We designed the front and back of the chassis with a curvature and shorter sides to allow for a larger approach angle on uneven terrains.

Our wheels feature a 3-spoke configuration and are machined from 150 µm thick FR4. We press fit the wheels onto the motor and bearing shafts to minimize the use of glue which could affect the motor shaft. Maximizing the wheel size for the motor spacing allowed by our chassis to provide up to 3 mm of clearance under the device, which is essential for navigating uneven terrain.

To design a robot with minimal size and actuators, we use only two of the low power vibration motors described above. To create a stable four wheel vehicle, we place ball bearings with 3 mm rods parallel to each motor. We orient the motors so that each side of the chassis has one motor-powered wheel and one free-spinning bearing wheel as seen in Fig 8. This arrangement allows us to power both motors simultaneously for straight movement or to power each motor individually for turning left or right, resulting in a highly maneuverable robot that can easily navigate in tight spaces. We manually assemble the components using cyanoacrylate adhesive.

3.5 Electronics and firmware

Next we design a power management and programmable control circuit to drive the robot. To minimize weight we create the circuit using a flexible 25 µm polyimide substrate clad on both sides with 12 um copper (AG122512EM). To minimize the robot's footprint, we designed the circuit to fold compactly for mounting onto the MilliMobile chassis. To fabricate the circuit, we coat both sides of the substrate in an etch resist and pattern traces with a laser (LPKF U4) before etching with ferric chloride to expose circuit features. High conductivity silver paint is applied to the board vias to ensure conductivity between board layers. After soldering the board components, we fold the circuit board to fit inside the robot chassis as shown in Fig 8.

The robot circuit is built around a programmable nRF52-series Bluetooth system-on-chip (SOC), which provides both low-power processing and Bluetooth communication. This is paired with a chip antenna (2450AT14A0100) with an additional 8 mm segment of 41 AWG wire to improve resonance at 2.4 GHz BLE bands. The PCB includes four photodiodes (SD019-141-411-R) to sample light intensity as well as a temperature and humidity sensor (HDC2010) to perform environmental monitoring tasks.

To operate with limited power harvesting sources, we design a power management circuit to distribute energy between the MCU and motors shown in Fig 9. To control the robot and perform sensing tasks, the circuit must first start its microcontroller. To perform cold-start from zero charge, we use the startup circuit from [11], but make additional modifications to manage the challenges of multiplexing a single solar/RF power harvester and balance the competing voltage requirements of our microcontroller and motors.

First, to minimize size and weight our robot only has a single RF or solar power harvester. We therefore add a switch to be able to toggle it between providing power to each component. When the circuit is powered off, the switch routes current from the harvester through the voltage regulator which acts as a voltage limiter and cold start circuitry to charge a small 7.5 mF supercapacitor. The startup circuit provides 1.9V power to the SOC once the capacitor voltage has risen to the supercapacitor's maximum voltage of 2.5V. Increasing the size of the storage capacitor C_{MCU} from [11] is critical to allow the MCU to remain ON while the switch charges the motor capacitors. This capacitor can run the MCU for 40 s to for operation in ultra-low light scenarios.

Second, this switch isolates the two voltage domains on our circuit. To keep our microcontroller ON while charging the motor capacitors, we seek to run our microcontroller at the lowest possible voltage to prevent a system brownout as C_{MCU} discharges. In contrast, our motor capacitors should be charged to a higher voltage to store more energy and enable greater motion per charging cycle. After powering on, the MCU triggers the switch to divert incoming power directly to the motor capacitors. Separating the power storage for the motors and the also allows us to select optimal capacitors to provide high peak current to the motors while selecting

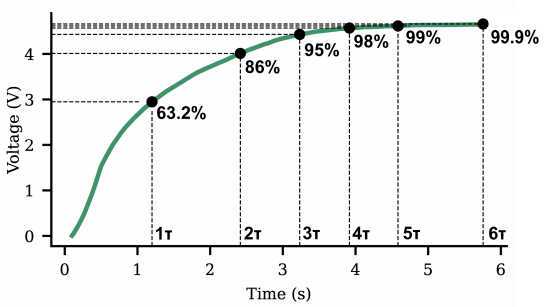

Figure 10: 150 µF capacitor charge curve versus time, with labeled Tau values and charge percentages.

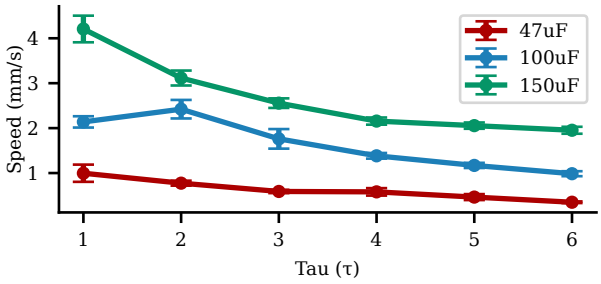

Figure 11: Indoor speed test under growlight set to 500 W/m^2 using a 1.2 g MilliMobile prototype.

a supercapacitor for the MCU with higher energy density for long-term operation. Additionally, powering the motors from a separate power source via transistors eliminates the risk of a system brownout from drawing high current from the high series resistance supercapacitor.

When configured to run off of harvested light energy, solar panels are connected directly to the input diode. When powered by harvested radio frequency (RF) power, a small wire antenna is connected to a rectifier with a voltage multiplier to generate a DC voltage. The rectifier breakout circuit occupies a similar footprint to the solar cell array, and the rectifier outputs are connected to the robot PCB input in place of the solar cells. This means that no additional changes to the main robot PCB are required when configuring for each of these power harvesting modes.

3.6 Optimizing Intermittent motion

The power output of harvesting sources often depends on the load connected to them. For example, a solar cell has a relatively flat I-V curve where it maintains a roughly constant open circuit voltage and then experiences a sharp drop off at the short circuit current. The cell therefore outputs maximum power $P = IV$ at the corner of this curve. The conventional approach to designing battery free systems is to use a power harvesting chip such as the TIBQ25570 to manage issues such as cold start described above and provide maximum power point tacking (MPPT) to operate the solar cells as close to this point as possible.

Dedicated power harvesting chips are however large and heavy and often require an off chip inductor to run their internal DC-DC converters. To minimize weight we instead connect our harvesting sources directly to the capacitors. This results in a changing charging rate over time.

The equation for a charging capacitor is: $V_c = V_{in}(1 - e^{(-t/\tau)})$, where V_c is the voltage across the capacitor, V_{in} is the harvester output, and τ is the time constant. The charge time is an exponential function and Fig 10 (measured data from our 47 µF capacitor with solar cells shown in Fig 4). The time constant τ depends on both the capacitance C of a capacitor of and resistance R of the circuit; it is the time it takes to reach 63.2% [16] of a final value, and we use τ as the point of comparison between capacitors in Fig 11.

For example, with a final voltage of 1V and capacitor values of 100 µF and 200 µF and a resistance of 50 Ω, the τ values are 5 ms and 10 ms, respectively. It would take the 100 µF capacitor 5 ms to reach 63.5% of 1V and the 200 µF capacitor 10 ms to reach 63.5% of 1V. A capacitor is considered fully charged after 5 τ values Fig 10 shows the percentage of charge at different tau values for a final charge of 5V.

If we seek to optimize our intermittent motion for speed, Fig 10 raises an important question: is there an optimal point of the curve in which to operate? For example the charging rate of the capacitor at 3 V is significantly faster than the charging rate at 5 V. Is it better to charge the capacitor for longer to move the MilliMobile further with each discharge, or to discharge the capacitor more frequently but travel a smaller distance each time? We perform a series of experiments below to determine an optimal charging time and use this to enable a novel *software defined MPPT*.

We evaluate the three capacitors from Fig 4 to observe the impact of τ charge times on robot speed. We first determined the τ values for each capacitor's charge and discharge curves and then incorporated these capacitors into the circuit for each motor. The device was then placed under a grow light with a light level 500 W/m^2 on top of black foam board material. We program a microcontroller to vary the τ values and measure the distance traveled by the robot using a ruler for 3 trials per τ value. Fig 11 shows the results and highlights interesting differences between the different capacitors. While longer charging times consistently decreases the speed for the 47 µF and 150 µF capacitors, the 100 µF capacitor exhibits an optimal value of 2τ. Based on this data we select the 150 µF capacitor and $\tau = 1$ for our final robot design.

3.7 Autonomous operation

The sections above address the issues of power autonomy by developing strategies to move our robot with harvested power. Fully autonomous operation however also requires sensing and control. Achieving all three pillars of autonomy for gram-scale robots has been a longstanding challenge in

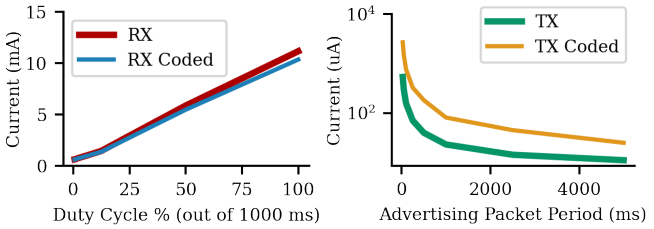

Figure 12: Left, current consumption of a nRF52840 in receiver mode with different scanning duty cycles. Right, power consumption of a nRF52840 in advertising mode with different packet transmit periods.

the microrobotics community [62]. Next, we build on our power harvesting results to augment our robot with sensing and control to demonstrate autonomous light seeking. In addition to serving as a demonstration of autonomy at this scale, light seeking enables our robots to find power sources.

To achieve this we equip the MilliMobile with four photodiodes in a reverse-bias configuration. The current across the diode increases along with light intensity, which results in a higher voltage measured by the ADC across a pulldown resistor. This allows the robot to sample the light intensity in each corner of the MilliMobile and identify the direction (front, back, left, or right) with the highest light intensity. Based on this information, the SOC triggers both motors to move forward, the left motor to turn left, or the right motor to turn right. In the case where the highest light intensity is in the back of the device, the robot turns right since it is only capable of driving the motors in the forward direction. In the default configuration, the MilliMobile samples the ADC channels once per second. However, in low power conditions the motor capacitor voltage may not be high enough to efficiently drive the motors. Because of this, the ADC also samples the voltage on each of the motor capacitors and executes a movement step if and only if the motor capacitors are charged above the optimal threshold voltage.

Algorithm 1 outlines this autonomous light-seeking behavior. Because the MilliMobile can harvest power from ambient light, light seeking is a particularly useful form of autonomy. By navigating towards locations with higher light intensity, the MilliMobile can increase the amount of harvested power and increase the available headroom for movement, data acquisition, and wireless networking tasks.

3.8 Wireless robotic networking

We leverage the Bluetooth functionality of the onboard nRF52 SOC to utilize the MilliMobile as a networked sensor node in addition to a robotics platform.

Transmitting data. Standard BLE devices consume several mA of current when transmitting and receiving data [29]. By duty cycling BLE advertising packets, we can throttle the data transmission rate based on available power and achieve average SOC power consumption as low as 11 µA

Algorithm 1 Light Seeking

```
if adc_motor_capacitors > V_threshold then
    front_intensity ← adc_front_right + adc_front_left
    left_intensity ← adc_front_left + adc_back_left
    right_intensity ← adc_front_right + adc_back_right
    back_intensity ← adc_back_left + adc_back_right
    if front_intensity == max_light_intensity then
        motor_left.pulse()
        motor_right.pulse()
    else if left_intensity == max_light_intensity then
        motor_left.pulse()
    else
        motor_right.pulse()
    end if
end if
```

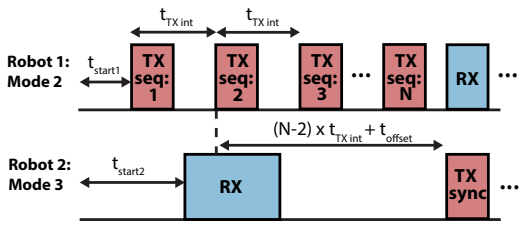

Figure 13: Multiple-Robot Synchronization protocol.

with a 0.2 Hz packet rate. We demonstrate two encoding schemes: standard BLE advertising using the 1M PHY, as well as Bluetooth Long Range advertising using the coded PHY on the nRF52840.

Receiving data. We also demonstrate the MilliMobile is able to act as a receiver to parse the advertising packets of other nearby MilliMobiles. However, operating the BLE radios in scan mode to detect incoming packets results in significantly higher power consumption than transmitting. Fig 12 compares measurements of the amount of power required to transmit and receive. When continuously scanning for incoming packets, the nRF52840 draws over 11 mA for standard mode and over 10 mA for coded-PHY mode. By implementing a short receive window as low as 2.5 ms, the average system power consumption for receiving in both PHY modes is approximately 650 µA.

Robot-to-robot communication. The highly asymmetric power requirements for transmitting and receiving impose significant challenges for communicating between robots and establishing a network of devices. To address this we propose a first of its kind battery-free robotic synchronization scheme that leverages the MilliMobile's photodiodes to seek out power for inter-robot communication. We leverage spatial variation in power to enable MilliMobiles harvesting large amounts of power act primarily in receive mode while devices with less available power operate primarily as transmitters. We describe the different modes of operation

Algorithm 2 Robot Synchronization

```
if I_thresh1 < I_in < I_thresh2 then
  for i ← 0, i < N do
    TX() {Send time to next RX window}
    i ← i + 1
    seek_light()
    while t < t_TXint do
      wait()
    end while
  end for
  RX() {Listen for synchronization packet}
else if I_in >= I_thresh2 then
  while t < RX_Window and !recieved do
    received_idx ← RX()
  end while
  if recieved then
    while t < (N − recieved_idx) * t_TXint + t_offset do
      wait()
    end while
    TX() {Send synchronization packet}
  else
    TX() {Send time to next RX window}
  end if
end if
```

for each robot in our synchronization method below which co-optimizes motion and wireless transmissions. Fig 13 illustrates the sequence of transmissions required to synchronize. This exploration of battery-free robot synchronization is a first step towards developing more complex and robust wireless protocols for battery-free robots, building on the significant prior works on battery-powered platforms [36, 67].

Mode 1: The MilliMobile begins in an ultra-low power state at startup sending an advertising packet with temperature data every 5 seconds. The device is programmed to move towards light, maximizing its power budget for motion.

Mode 2: Upon reaching a harvested current of $I_{thresh1}$ the robot enters Mode 2 and sends a series of N packets at a faster fixed time interval as shown in Fig 13. Each packet encodes a sequence number. After transmitting N packets, the robot enters a brief RX window to receive a timing synchronization packet. The robot continues seeking light but uses a larger portion of its power budget for communication.

Mode 3: When a MilliMobile detects higher input current above $I_{thresh2}$, it enters Mode 3 operation. In Mode 3, the robot stops moving and scans for advertising packets for a time period greater the Mode 2 advertising frequency. This ensures it is able to receive at least one packet from nearby Mode 2 robots. The Mode 3 robot decodes the packet to determine the amount of time remaining until the nearby Mode 2 robot enters its RX window. The Mode 3 robot sets a timer and sends a short synchronization packet to align with the detected robot's RX window.

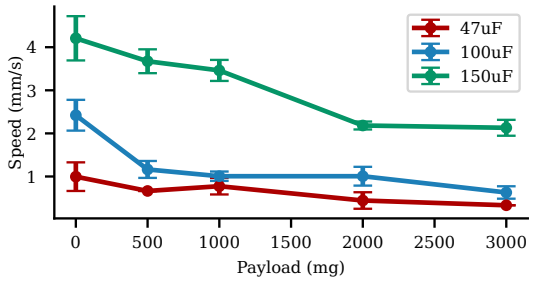

Figure 14: Speed versus payload test using a 1.2 g MilliMobile and a 1 Tau charge time, performed indoors under 500 W/m^2 light using various capacitors.

Upon receiving the packet, the Mode 2 and Mode 3 robots can both set timers to continue exchanging packets at a longer time interval. To handle the case where both robots are in Mode 3, if no Mode 2 packets are received the Mode 3 robot will also transmit a single advertisement containing the equivalent cycles remaining until it enters the receive state so it can capture a transmission sync from another Mode 3 robot. Pseudocode for this process is shown in Algorithm 2.

To verify this protocol is compatible with our battery-free circuit, we perform power measurements to verify the maximum time windows and thresholds required. We demonstrate the stability of this protocol with Mode 3 receive windows up to 50 ms every 2 seconds resulting in an $I_{thresh2}$ = 1000 µA and corresponding Mode 2 transmissions every 45 ms resulting in an $I_{thresh1}$ = 250 µA. Once synchronized, a receive window of 2.5 ms is required to reliably capture a single transmitted advertising packet. The ability to perform bi-directional communication can allow one robot to coordinate transmissions in a TDMA scheme or allow a node with higher power to serve as a relay to a base station.

We demonstrate a novel approach to device synchronization that leverages the robot's ability to move. We note that this simple protocol is a demonstration of our platform's capabilities could be further optimized and extended in future work to enable networking among multiple robots.

4 RESULTS

4.1 Robot performance

We evaluate the end-to-end performance of our robot below including the effects of payload, power harvested, and terrain. We perform all tests with the same chassis and drive circuit, but vary the capacitor size which we specify for each experiment below. To test the payload capacity of our device, we varied the weight from 0 to 3000 mg, which is almost a 3x increase in weight from the lightest version of our device. Using the optimal τ for each capacitor that produced the best

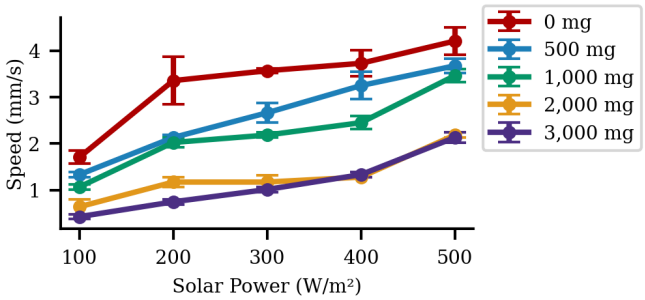

Figure 15: Speed versus solar power test using a 1.2 g MilliMobile, 150 µF capacitor, and a 1 Tau charge time, performed indoors carrying various payloads.

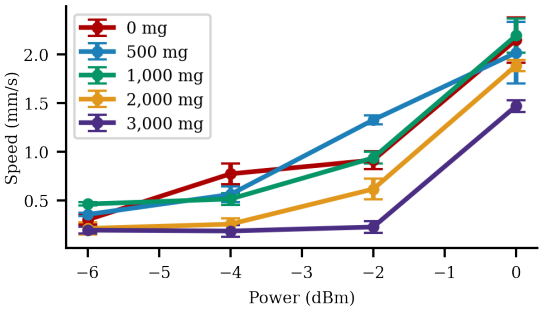

Figure 16: Speed versus RF power test using a 1.2 g MilliMobile, 150 µF capacitor, and 1 Tau charge time, performed indoors carrying various payloads.

speeds and the same setup from Fig 11, we measured the speed of our device for each weight, as shown in Fig 14. At a solar power density of 500 W/m^2, the device with the 150 µF capacitor achieved the best speed for any given payload.

The ability for our robot to carry 3 times its own weight also highlights the high torque generated by the pulsed ERM motors. In some cases, adding weight assisted in translating the motor torque to forward motion, increasing the friction between the wheels and the ground and preventing excess wheelspin. The MilliMobile can carry up to 1,000 mg of payload while only suffering a 25% reduction in speed with the 150 µF capacitor, demonstrating that our device can carry significant additional payloads by trading off overall speed.

We also test the effect of solar power on speed using the same test setup with different payloads to show the ability to carry additional devices and sensors. Fig 15 shows the five curves that depict the device's speed at a given solar profile and weight. As weight increases, speed decreases significantly, especially at lower light intensities.

Fig 16 demonstrates the effects of RF power on the speed of the device with different payloads. The harvesting circuit generally exhibited lower speed results than the solar setup, due to lower power levels tested and corresponding lower voltage outputs. In both cases, we found that increased power increased our speed while adding weight decreased speed.

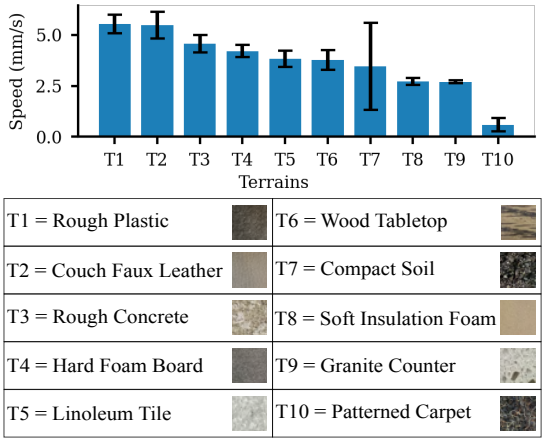

Figure 17: Speed versus terrain test using a 1.2 g MilliMobile, a 150 µF capacitor, and a 1 Tau charge time.

We note that even at -6 dBm when receiving less than 50 µW of power, our robot was able to move forward demonstrating the ability of intermittent motion to scale to very low input powers. Additionally, our robot can successfully cold-start with as little as 7 uA enabling operation in a wide variety of light conditions, including indoor lighting.

In addition to evaluating the effect of power harvesting on speed, we also characterize the robot's speed on 10 different types of terrain in Fig 17. For each test, we used the 150 µF capacitor at $\tau = 1$ for the charge and discharge cycles. We conducted all trials under a grow light that provided a light intensity of 500 W/m^2 to the MilliMobile's solar cells. We ran three trials per terrain.

The device was most effective on rough plastic material and a leather material T1 and T2, respectively, in the table in Fig 17. The device had reduced performance on surfaces such as granite countertops and patterned carpets. We believe that the device performed poorly on these surfaces due to the low friction from the wheel and the low weight of its design which does not perform well on very slippery or smooth surfaces. A solution to this would be to add additional weight or increase the friction of the wheel by either adding a rubber coating or increasing the contact area of the wheel. On certain types of carpet, the large fibers increased the probability that the device would get lifted on one of those fibers, and the motor did not make full contact with the ground. One solution to this would be to increase the diameter of the wheel to allow for more chassis ground clearance and avoid being lifted by the fibers. Overall, the device's performance on different terrains was comparable to its performance on hard foam board used for the results in Fig 11, Fig 14, Fig 15, and Fig 16.

By characterizing the best capacitor, payload, solar/RF condition, and operable terrains, we can tune the MilliMobile to operate in a variety of environmental conditions. For example, to quickly gather many sensor readings in a bright

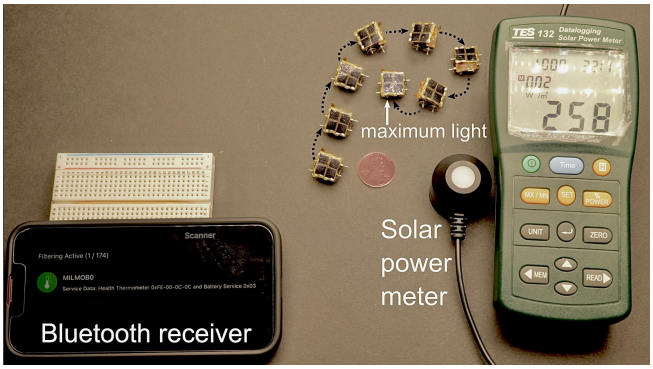

Figure 18: Autonomous operation with onboard solar harvesting circuit gathering 232 µA in 258 W/m^2, while broadcasting data via Bluetooth at 1 Hz.

outdoor environment we can take advantage of the payload headroom to utilize larger capacitors as well as incorporate additional sensors. In the case of indoor operation where travel distance and speed are lower priority, we can attach smaller capacitors for faster charge time in low-power conditions while simultaneously saving weight by reducing the number of onboard sensors.

4.2 Evaluating autonomous operation

We evaluate our autonomous light seeking described above. Fig 18 shows the robot moving toward the region with maximum light on a foam board. In maximum light, the onboard solar cells brightly reflect the light from a grow light placed approximately 40 cm above the foam board.

We further evaluated the MilliMobile's light seeking performance at a hydroponic farm. Fig 19 shows the MilliMobile reorienting itself toward the direction of maximum light on a rough plastic surface. Within 13 s the MilliMobile is able to spin approximately 180°, before continuing forward toward the location of maximum detected light.

4.3 Wireless evaluation

We evaluate the wireless range of our MilliMobile in outdoor environments using our small form factor onboard antenna in Fig 20. We first evaluate sending long-range coded packets to a base station equipped with a 8 dBi, 2.4 GHz patch antenna (L-COM RE09P-SM). We program the onboard BLE chip to transmit 300 advertising packets from the MilliMobile antenna and count the number received by the base station. With this setup, we observe a packet delivery rate of 81% at 100 m and a packet delivery rate of 9% at 700 m. This demonstrates the ability of the MilliMobile to successfully transmit packets over a range of several hundred meters, enabling practical real-world deployments over large areas.

We also evaluated the RF performance of peer-to-peer packet transmission by using the MilliMobile antenna on both the transmitting and receiving end of the test setup.

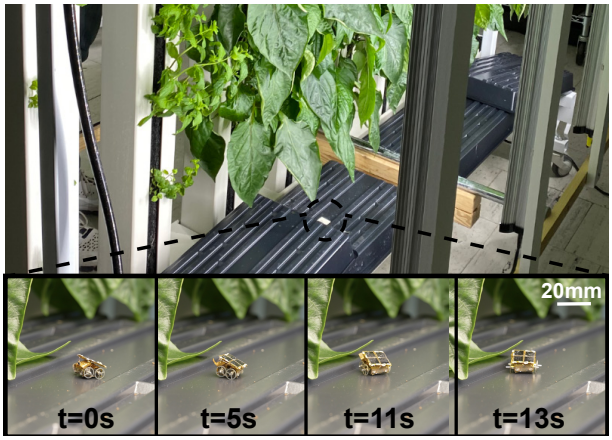

Figure 19: Battery-free and wireless MilliMobile operation at the bottom of a hydroponic farm. The solar cells onboard harvest power from nearby grow lights.

In this configuration, the MilliMobile is able to send and receive long-range coded packets at a range of 140 m and standard BLE advertising packets at up to 40 m. Although limited by losses of the small form-factor antenna, this range still allows for robust inter-device communication in dense deployment.

5 DISCUSSION AND CONCLUSION

This paper presents MilliMobile, a first of its kind battery free autonomous robot. We challenge the conventional assumption that motion and actuation are beyond the capabilities of battery free devices and demonstrate completely untethered autonomous operation in realistic lighting and RF power delivery scenarios using intermittent motion to move with as little as 57 µW of power. Our gram-scale robot demonstrates power, sensor, and control autonomy as well as wireless connectivity. We discuss potential applications, limitations, and future directions below.

Sensor payloads. Our robot can carry 3 times its own weight and support a wide variety of sensor payloads. Fig 21 shows commercially available sensors compatible with our robot. We note that many of these weigh less than 100 mg demonstrating potential for integrating sensor payloads with minimal impact on speed. Fig 14 however demonstrates that our robot can carry heavier payloads such as a CO2 sensor.

Robot application scenarios. The ability to carry a wide variety of sensor payloads enables numerous application scenarios. In comparison to a static sensor node, MilliMobile can actively seek out and localize sensory signals. For example, MilliMobile could seek out gas or chemical leaks using gas sensors, metal objects with a magnetometer, RF sources using an antenna and receiver or envelope detector, temperature for detecting fires or sources of heat, and much more. The ability to move also enables sampling of

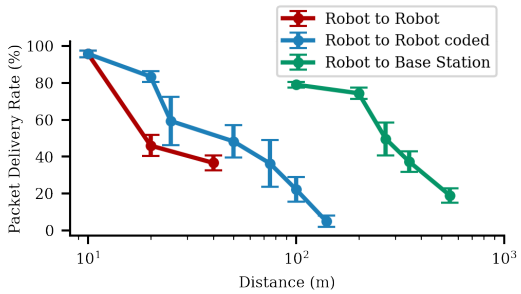

Figure 20: BLE packet delivery rate versus distance. Experiments conducted using radios with sensitivities of -95 dBm (-103 dBm coded PHY), with -0.5 dBi antennas on MilliMobile and 8 dBi antennas at base station.

Sensor	Part Number	Mass (mg)	Power (µW)
Photoresistor	ALS-PT19-315C_L177_TR8	1.35	0.6
Magnetometer	MMC5633NJL	0.8	33.18
Pressure + Temperature	BMP384	7.0	6.12
Humidity + Temperature	HDC2010YPAT	2.65	111.4
Air Quality + Humidity + Pressure + Temperature	BMP688	16.0	162.0
CO2 sensor	SCD41	600	400
Camera	HM01B0	24.0	2,000.0

Figure 21: Mass and power measurements for additional sensors compatible with the power and weight constraints of our MilliMobile robot.

spatial gradients which is important for many of these applications. When combined with sensors like cameras, our robots could be used to automate a wide variety of inspection tasks, especially in scenarios dangerous to humans.

Industrial equipment and infrastructure such as high powered radio transmitters and other devices that generate strong electromagnetic fields are harmful to human health, but provides the perfect scenario for power harvesting robots to automate dangerous tasks. Our robots are not constrained by battery life and could in theory operate for infinite lifetimes outdoors for inspection tasks on roads, railroad tracks, etc. Similarly our robots could be used for space or interplanetary exploration due to their small size and ability to operate on harvested energy. The ability to move in such a small form factor could also be combined with recent developments in airborne sensor release [11, 28, 47, 57] to enable precise large scale deployment of sensor networks.

Battery free actuation. The ability to perform battery-free actuation opens up a variety of new research directions for low power wireless systems. For example, the ability to move a whole sensor node or parts of it permits incorporating remote feedback from an edge device to create a dynamically controllable sensor network. For example, a base station could coordinate the network to steer directional sensors such as cameras to focus on a sensing target of interest, or nodes could use this ability to move themselves or their antenna to optimize connectivity. These same principles could also be extended to other domains as well such as HCI to enable battery-free haptic interfaces. Our robot uses vibration motors which are designed for haptic interfaces. Additionally these techniques could be extended to use other actuators such as solenoids or piezos and combined with alternative energy harvesting modalities such as harvesting power from button presses or user motion for wearables.

Improving power harvesting. Improving the power harvesting of our robot could further improve performance. A custom circuit with maximum power point tracking (MPPT) and boost converter could be used to increase efficiency in high payload scenarios, and combining RF and solar harvesting could further increase power delivery. Multi-band power harvesting, beamforming to specific nodes, and improved antennas could further improve RF harvesting.

Robot autonomy and networking. While our robot is capable of moving towards a target like a light source, it currently lacks navigation and feedback control. Integrating an accelerometer or employing some of the many wireless localization techniques developed by the mobile systems community could enable the robots to travel to precise locations [4, 52]. Additionally there are significant opportunities to improve networking capabilities that establish connectivity between nodes to enable large scale swarms of robotic sensor nodes [36, 67].

6 ACKNOWLEDGMENTS

We thank Chun-Cheng Chang and Raul Villanueva for help with experiments and preparing demos. This research was partially supported by an Amazon Research Award, a Google Research Scholar Award, the National Science Foundation Graduate Research Fellowship Program, the National GEM Consortium Fellowship Program, the Washington NASA Space Grant Consortium Fellowship Program, the Pastry-Powered T(o)uring Machine Endowed Fellowship, and the SPEEA ACE Fellowship Program.

REFERENCES

[1] 2017. Motor Brushed 4mm x 12mm 7 Ohm (Pack of 3). https://micronwings.com/product/motor-brushed-4mm-x-12mm-7-ohm-pack-of-3/.

[2] M. C. Achtelik, J. Stumpf, D. Gurdan, and K. M. Doth. 2011. Design of a flexible high performance quadcopter platform breaking the MAV endurance record with laser power beaming. In *2011 IEEE/RSJ International Conference on Intelligent Robots and Systems*. 5166–5172. https://doi.org/10.1109/IROS.2011.6094731

[3] Vicente Arroyos, Maria LK Viitaniemi, Nicholas Keehn, Vaidehi Oruganti, Winston Saunders, Karin Strauss, Vikram Iyer, and Bichlien H Nguyen. 2022. A Tale of Two Mice: Sustainable Electronics Design and Prototyping. In *CHI Conference on Human Factors in Computing*

Systems Extended Abstracts. 1–10.

[4] Roshan Ayyalasomayajula, Deepak Vasisht, and Dinesh Bharadia. 2018. BLoc: CSI-Based Accurate Localization for BLE Tags. In *Proceedings of the 14th International Conference on Emerging Networking EXperiments and Technologies* (Heraklion, Greece) *(CoNEXT '18)*. Association for Computing Machinery, 126–138.

[5] Palak Bhushan and Claire Tomlin. 2020. Design of an electromagnetic actuator for an insect-scale spinning-wing robot. *IEEE Robotics and Automation Letters* 5, 3 (2020), 4188–4193.

[6] P. Bhushan and C. Tomlin. 2020. An Insect-Scale Self-Sufficient Rolling Microrobot. *IEEE Robotics and Automation Letters* 5, 1 (2020), 167–172.

[7] Cindy S Bick, Inhee Lee, Trevor Coote, Amanda E Haponski, David Blaauw, and Diarmaid Ó Foighil. 2021. Millimeter-sized smart sensors reveal that a solar refuge protects tree snail Partula hyalina from extirpation. *Communications Biology* 4, 1 (2021), 744.

[8] G. Caprari, P. Balmer, R. Piguet, and R. Siegwart. 1998. The autonomous micro robot "Alice": a platform for scientific and commercial applications. In *MHA'98. Proceedings of the 1998 International Symposium on Micromechatronics and Human Science. - Creation of New Industry - (Cat. No.98TH8388)*. 231–235. https://doi.org/10.1109/MHS.1998.745787

[9] Yogesh M Chukewad, Avinash T Singh, Johannes M James, and Sawyer B Fuller. 2018. A new robot fly design that is easier to fabricate and capable of flight and ground locomotion. *2018 IEEE/RSJ International Conference on Intelligent Robots and Systems (IROS)* (2018), 4875–4882.

[10] Alexei Colin, Emily Ruppel, and Brandon Lucia. 2018. A Reconfigurable Energy Storage Architecture for Energy-Harvesting Devices. *SIGPLAN Not.* 53, 2 (mar 2018), 767–781. https://doi.org/10.1145/3296957.3173210

[11] Cathal Cummins, Madeleine Seale, Alice Macente, Daniele Certini, Enrico Mastropaolo, and Naomi Nakayama. 2018. A separated vortex ring underlies the flight of the dandelion. *Nature* 562 (10 2018). https://doi.org/10.1038/s41586-018-0604-2

[12] Alexander Curtiss, Blaine Rothrock, Abu Bakar, Nivedita Arora, Jason Huang, Zachary Englhardt, Aaron-Patrick Empedrado, Chixiang Wang, Saad Ahmed, Yang Zhang, et al. 2021. FaceBit: Smart face masks platform. *Proceedings of the ACM on Interactive, Mobile, Wearable and Ubiquitous Technologies* 5, 4 (2021), 1–44.

[13] Jasper de Winkel, Carlo Delle Donne, Kasim Sinan Yildirim, Przemysław Pawełczak, and Josiah Hester. 2020. Reliable timekeeping for intermittent computing. In *Proceedings of the Twenty-Fifth International Conference on Architectural Support for Programming Languages and Operating Systems*. 53–67.

[14] Jasper De Winkel, Haozhe Tang, and Przemysław Pawełczak. 2022. Intermittently-powered bluetooth that works. In *Proceedings of the 20th Annual International Conference on Mobile Systems, Applications and Services*. 287–301.

[15] Bardienus P. Duisterhof, Shushuai Li, Javier Burgués, Vijay Janapa Reddi, and Guido C. H. E. de Croon. 2021. Sniffy Bug: A Fully Autonomous Swarm of Gas-Seeking Nano Quadcopters in Cluttered Environments. In *2021 IEEE/RSJ International Conference on Intelligent Robots and Systems (IROS)*. 9099–9106. https://doi.org/10.1109/IROS51168.2021.9636217

[16] ElectricTutorials. [n. d.]. Tau – The Time Constant.

[17] N. Elkunchwar, K. Balasubramanian, J. Noe, M. Anderson, and S. B. Fuller. [n. d.]. Simultaneous source seeking and obstacle avoidance on a palm-sized drone. ([n. d.]). under review.

[18] Nishant Elkunchwar, Suvesha Chandrasekaran, Vikram Iyer, and Sawyer B Fuller. [n. d.]. Toward battery-free flight: Duty cycled recharging of small drones. In *2021 IEEE/RSJ International Conference on Intelligent Robots and Systems (IROS)*. IEEE, 5234–5241.

[19] Hector D. Escobar-Alvarez, Neil Johnson, Tom Hebble, Karl Klingebiel, Steven A. P. Quintero, Jacob Regenstein, and N. Andrew Browning. 2018. R-ADVANCE: Rapid Adaptive Prediction for Vision-based Autonomous Navigation, Control, and Evasion. *Journal of Field Robotics* 35, 1 (2018), 91–100. https://doi.org/10.1002/rob.21744

[20] Kai Geissdoerfer and Marco Zimmerling. 2021. Bootstrapping Battery-free Wireless Networks: Efficient Neighbor Discovery and Synchronization in the Face of Intermittency.. In *NSDI*, Vol. 21. 439–455.

[21] Benjamin Goldberg, Raphael Zufferey, Neel Doshi, Elizabeth Farrell Helbling, Griffin Whittredge, Mirko Kovac, and Robert J. Wood. 2018. Power and Control Autonomy for High-Speed Locomotion With an Insect-Scale Legged Robot. *IEEE Robotics and Automation Letters* 3, 2 (2018), 987–993. https://doi.org/10.1109/LRA.2018.2793355

[22] Benjamin Goldberg, Raphael Zufferey, Neel Doshi, Elizabeth Farrell Helbling, Griffin Whittredge, Mirko Kovac, and Robert J. Wood. 2018. Power and Control Autonomy for High-Speed Locomotion With an Insect-Scale Legged Robot. *IEEE Robotics and Automation Letters* 3, 2 (2018), 987–993. https://doi.org/10.1109/LRA.2018.2793355

[23] Seth Hollar, Anita Flynn, Colby Bellew, and KSJ Pister. 2003. Solar powered 10 mg silicon robot. In *The Sixteenth Annual International Conference on Micro Electro Mechanical Systems, 2003. MEMS-03 Kyoto. IEEE.* IEEE, 706–711.

[24] Aaron M Hoover, Erik Steltz, and Ronald S Fearing. 2008. RoACH: An autonomous 2.4 g crawling hexapod robot. *2008 IEEE/RSJ International Conference on Intelligent Robots and Systems* (2008), 26–33.

[25] Rudolf Yoga Hutama, Mohamed M Khalil, and Tomoaki Mashimo. 2021. A millimeter-scale rolling microrobot driven by a micro-geared ultrasonic motor. *IEEE Robotics and Automation Letters* 6, 4 (2021), 8158–8164.

[26] Vikram Iyer, Elyas Bayati, Rajalakshmi Nandakumar, Arka Majumdar, and Shyamnath Gollakota. 2018. Charging a smartphone across a room using lasers. *Proceedings of the ACM on Interactive, Mobile, Wearable and Ubiquitous Technologies* 1, 4 (2018), 1–21.

[27] Vikram Iyer, Maruchi Kim, Shirley Xue, Anran Wang, and Shyamnath Gollakota. 2020. Airdropping sensor networks from drones and insects. 1–14. https://doi.org/10.1145/3372224.3419981

[28] Vikram Iyer, Maruchi Kim, Shirley Xue, Anran Wang, and Shyamnath Gollakota. 2020. Airdropping Sensor Networks from Drones and Insects. *Proceedings of the 26th Annual International Conference on Mobile Computing and Networking*, Article 61 (2020), 14 pages. https://doi.org/10.1145/3372224.3419981

[29] Vikram Iyer, Ali Najafi, Johannes James, Sawyer Fuller, and Shyamnath Gollakota. 2020. Wireless steerable vision for live insects and insect-scale robots. *Science Robotics* 5, 44 (2020). https://doi.org/10.1126/scirobotics.abb0839

[30] Vikram Iyer, Rajalakshmi Nandakumar, Anran Wang, Sawyer B. Fuller, and Shyamnath Gollakota. 2019. Living IoT: A Flying Wireless Platform on Live Insects. *The 25th Annual International Conference on Mobile Computing and Networking* (2019), 1–15. https://doi.org/10.1145/3300061.3300136

[31] Noah Jafferis, E. Helbling, Michael Karpelson, and Robert Wood. 2019. Untethered flight of an insect-sized flapping-wing microscale aerial vehicle. *Nature* 570 (2019). https://doi.org/10.1038/s41586-019-1322-0

[32] Noah T Jafferis, E Farrell Helbling, Michael Karpelson, and Robert J Wood. 2019. Untethered flight of an insect-sized flapping-wing microscale aerial vehicle. *Nature* 570, 7762 (2019), 491.

[33] Johannes James, Vikram Iyer, Yogesh Chukewad, Shyamnath Gollakota, and Sawyer B Fuller. 2018. Liftoff of a 190 mg laser-powered aerial vehicle: The lightest wireless robot to fly. *2018 IEEE International Conference on Robotics and Automation (ICRA)* (2018), 1–8.

[34] Xiaobin Ji, Xinchang Liu, Vito Cacucciolo, Matthias Imboden, Yoan Civet, Alae El Haitami, Sophie Cantin, Yves Perriard, and Herbert

Shea. 2019. An autonomous untethered fast soft robotic insect driven by low-voltage dielectric elastomer actuators. *Science Robotics* 4, 37 (2019).

[35] Yujiro Kakei, Shumpei Katayama, Shinyoung Lee, Masahito Takakuwa, Kazuya Furusawa, Shinjiro Umezu, Hirotaka Sato, Kenjiro Fukuda, and Takao Someya. 2022. Integration of body-mounted ultrasoft organic solar cell on cyborg insects with intact mobility. *npj Flexible Electronics* 6, 1 (2022), 78.

[36] Arvind Kandhalu, Karthik Lakshmanan, and Ragunathan (Raj) Rajkumar. 2010. U-Connect: A Low-Latency Energy-Efficient Asynchronous Neighbor Discovery Protocol. In *Proceedings of the 9th ACM/IEEE International Conference on Information Processing in Sensor Networks* (Stockholm, Sweden) *(IPSN '10)*. Association for Computing Machinery, New York, NY, USA, 350–361. https://doi.org/10.1145/1791212.1791253

[37] Daniel Hsing Po Kang, Mengjun Chen, and Oladele A Ogunseitan. 2013. Potential environmental and human health impacts of rechargeable lithium batteries in electronic waste. *Environmental science & technology* 47, 10 (2013), 5495–5503.

[38] Michael Karpelson, Benjamin H Waters, Benjamin Goldberg, Brody Mahoney, Onur Ozcan, Andrew Baisch, Pierre-Marie Meyitang, Joshua R Smith, and Robert J Wood. 2014. A wirelessly powered, biologically inspired ambulatory microrobot. In *2014 IEEE International Conference on Robotics and Automation (ICRA)*. IEEE, 2384–2391.

[39] Peter J Kennedy, Scott M Ford, Juliette Poidatz, Denis Thiéry, and Juliet L Osborne. 2018. Searching for nests of the invasive Asian hornet (Vespa velutina) using radio-telemetry. *Communications biology* 1, 1 (2018), 88.

[40] Bong Hoon Kim, Kan Li, Jin-Tae Kim, Yoonseok Park, Hokyung Jang, Xueju Wang, Zhaoqian Xie, Sang Min Won, Hong-Joon Yoon, Geumbee Lee, et al. 2021. Three-dimensional electronic microfliers inspired by wind-dispersed seeds. *Nature* 597, 7877 (2021), 503–510.

[41] Yongdeok Kim, Yiyuan Yang, Xiaotian Zhang, Zhengwei Li, Abraham Vázquez-Guardado, Insu Park, Jiaojiao Wang, Andrew I. Efimov, Zhi Dou, Yue Wang, Junehu Park, Haiwen Luan, Xinchen Ni, Yun Seong Kim, Janice Baek, Joshua Jaehyung Park, Zhaoqian Xie, Hangbo Zhao, Mattia Gazzola, John A. Rogers, and Rashid Bashir. 2023. Remote control of muscle-driven miniature robots with battery-free wireless optoelectronics. *Science Robotics* 8, 74 (2023), eadd1053. https://doi.org/10.1126/scirobotics.add1053

[42] Inhee Lee, Roger Hsiao, Gordy Carichner, Chin-Wei Hsu, Mingyu Yang, Sara Shoouri, Katherine Ernst, Tess Carichner, Yuyang Li, Jaechan Lim, et al. 2021. mSAIL: milligram-scale multi-modal sensor platform for monarch butterfly migration tracking. In *Proceedings of the 27th Annual International Conference on Mobile Computing and Networking*.

[43] Jiaming Liang, Yichuan Wu, Justin K Yim, Huimin Chen, Zicong Miao, Hanxiao Liu, Ying Liu, Yixin Liu, Dongkai Wang, Wenying Qiu, et al. 2021. Electrostatic footpads enable agile insect-scale soft robots with trajectory control. *Science Robotics* 6, 55 (2021), eabe7906.

[44] Chris Looney, Brant Carman, Jenni Cena, Cassie Cichorz, Vikram Iyer, Jessica Orr, Nathan Roueché, Karla Salp, Jacqueline M Serrano, Landon Udo, et al. 2023. Detection and description of four Vespa mandarinia (Hymenoptera, Vespidae) nests in western North America. *Journal of Hymenoptera Research* 96 (2023), 1–20.

[45] Haojian Lu, Ying Hong, Yuanyuan Yang, Zhengbao Yang, and Yajing Shen. 2020. Battery-Less Soft Millirobot That Can Move, Sense, and Communicate Remotely by Coupling the Magnetic and Piezoelectric Effects. *Advanced Science* 7, 13 (2020), 2000069. https://doi.org/10.1002/advs.202000069

[46] Guo Zhan Lum, Zhou Ye, Xiaoguang Dong, Hamid Marvi, Onder Erin, Wenqi Hu, and Metin Sitti. 2016. Shape-programmable magnetic soft matter. *Proceedings of the National Academy of Sciences* 113, 41 (2016).

[47] Danli Luo, Aditi Maheshwari, Andreea Danielescu, Jiaji Li, Yue Yang, Ye Tao, Lingyun Sun, Dinesh K Patel, Guanyun Wang, Shu Yang, et al. 2023. Autonomous self-burying seed carriers for aerial seeding. *Nature* 614, 7948 (2023), 463–470.

[48] Kevin Y Ma, Pakpong Chirarattananon, Sawyer B Fuller, and Robert J Wood. 2013. Controlled flight of a biologically inspired, insect-scale robot. *Science* 340, 6132 (2013), 603–607.

[49] James McLurkin and Jennifer Smith. 2007. Distributed Algorithms for Dispersion in Indoor Environments Using a Swarm of Autonomous Mobile Robots. In *Distributed Autonomous Robotic Systems 6*, Rachid Alami, Raja Chatila, and Hajime Asama (Eds.). Springer Japan, Tokyo, 399–408.

[50] Shuhei Miyashita, Steven Guitron, Marvin Ludersdorfer, Cynthia R Sung, and Daniela Rus. 2015. An untethered miniature origami robot that self-folds, walks, swims, and degrades. *2015 IEEE International Conference on Robotics and Automation (ICRA)* (2015), 1490–1496.

[51] Shuhei Miyashita, Steven Guitron, Kazuhiro Yoshida, Shuguang Li, Dana D Damian, and Daniela Rus. 2016. Ingestible, controllable, and degradable origami robot for patching stomach wounds. *2016 IEEE international conference on robotics and automation (ICRA)* (2016), 909–916.

[52] Rajalakshmi Nandakumar, Vikram Iyer, and Shyamnath Gollakota. 2018. 3D Localization for Sub-Centimeter Sized Devices. *SenSys* (2018), 12 pages. https://doi.org/10.1145/3274783.3274851

[53] NASA. 2004. Laser power for UAVs.

[54] Takashi Ozaki, Norikazu Ohta, Tomohiko Jimbo, and Kanae Hamaguchi. 2021. A wireless radiofrequency-powered insect-scale flapping-wing aerial vehicle. *Nature Electronics* 4, 11 (2021), 845–852.

[55] Ryan St Pierre and Sarah Bergbreiter. 2016. Gait exploration of sub-2 g robots using magnetic actuation. *IEEE Robotics and Automation Letters* 2, 1 (2016), 34–40.

[56] Paul Pounds, Timothy Potie, Farid Kendoul, Surya Singh, Raja Jurdak, and Jonathan Roberts. 2014. Automatic Distribution of Disposable Self-Deploying Sensor Modules, Vol. 109. https://doi.org/10.1007/978-3-319-23778-7_35

[57] P. Pounds and S. Singh. 2015. Samara: Biologically Inspired Self-Deploying Sensor Networks. *IEEE Potentials* 34, 2 (March 2015), 10–14. https://doi.org/10.1109/MPOT.2014.2359034

[58] Michael F Reynolds, Alejandro J Cortese, Qingkun Liu, Zhangqi Zheng, Wei Wang, Samantha L Norris, Sunwoo Lee, Marc Z Miskin, Alyosha C Molnar, Itai Cohen, et al. 2022. Microscopic robots with onboard digital control. *Science Robotics* 7, 70 (2022), eabq2296.

[59] Michael Rubenstein, Christian Ahler, Nick Hoff, Adrian Cabrera, and Radhika Nagpal. 2014. Kilobot: A low cost robot with scalable operations designed for collective behaviors. *Robotics and Autonomous Systems* 62, 7 (2014), 966–975.

[60] Michael Rubenstein, Christian Ahler, and Radhika Nagpal. 2012. Kilobot: A low cost scalable robot system for collective behaviors. *2012 IEEE International Conference on Robotics and Automation* (2012), 3293–3298.

[61] Metta Santiputri and Muhammad Tio. 2018. IoT-based Gas Leak Detection Device. In *2018 International Conference on Applied Engineering (ICAE)*. 1–4. https://doi.org/10.1109/INCAE.2018.8579396

[62] Ryan St. Pierre and Sarah Bergbreiter. 2019. Toward Autonomy in Sub-Gram Terrestrial Robots. *Annual Review of Control, Robotics, and Autonomous Systems* 2, 1 (2019), 231–252. https://doi.org/10.1146/annurev-control-053018-023814 arXiv:https://doi.org/10.1146/annurev-control-053018-023814

[63] Vamsi Talla, Bryce Kellogg, Benjamin Ransford, Saman Naderiparizi, Shyamnath Gollakota, and Joshua R. Smith. 2015. Powering the Next Billion Devices with Wi-fi. *Proceedings of the 11th ACM Conference on Emerging Networking Experiments and Technologies*, Article 4 (2015),

13 pages. https://doi.org/10.1145/2716281.2836089

[64] Michael M Thackeray, Christopher Wolverton, and Eric D Isaacs. 2012. Electrical energy storage for transportation—approaching the limits of, and going beyond, lithium-ion batteries. *Energy & Environmental Science* 5, 7 (2012), 7854–7863.

[65] Laurent Vandepaer, Julie Cloutier, and Ben Amor. 2017. Environmental impacts of Lithium Metal Polymer and Lithium-ion stationary batteries. *Renewable and Sustainable Energy Reviews* 78 (2017), 46–60.

[66] Dana Vogtmann, Ryan St Pierre, and Sarah Bergbreiter. 2017. A 25 mg magnetically actuated microrobot walking at> 5 body lengths/sec. In *2017 IEEE 30th International Conference on Micro Electro Mechanical Systems (MEMS)*. IEEE, 179–182.

[67] Shuai Wang, Jianlin Guo, Pu Wang, Kieran Parsons, Philip Orlik, Yukimasa Nagai, Takenori Sumi, and Parth Pathak. 2022. X-Disco: Cross-technology Neighbor Discovery. In *2022 19th Annual IEEE International Conference on Sensing, Communication, and Networking (SECON)*. 163–171. https://doi.org/10.1109/SECON55815.2022.9918568

[68] Tony Wang, Daasol Yang, Jiehao Chen, Jocelyn Chow, Yuhang Hu, Kimberly Hoang, and Azadeh Ansari. 2022. A Tetherless Microdriller for Maneuverability and On-Board Cargo Delivery Inside Viscoelastic Media. In *2022 International Conference on Manipulation, Automation and Robotics at Small Scales (MARSS)*. IEEE, 1–6.

[69] Robert J Wood. 2008. The first takeoff of a biologically inspired at-scale robotic insect. *IEEE transactions on robotics* 24, 2 (2008), 341–347.

[70] Yichuan Wu, Justin K Yim, Jiaming Liang, Zhichun Shao, Mingjing Qi, Junwen Zhong, Zihao Luo, Xiaojun Yan, Min Zhang, Xiaohao Wang, et al. 2019. Insect-scale fast moving and ultrarobust soft robot. *Science robotics* 4, 32 (2019), eaax1594.